Emx1-Cre is expressed in vagal afferent nerves that regulate central cardiorespiratory functions

Isamu Aiba*, Yao Ning, Jeffery L. Noebels

Department of Neurology, Baylor College of Medicine, Houston Texas 77030

*Correspondence: Isamu Aiba (email: aiba@bcm.edu)

Abstract

The Emx1-IRES-Cre transgenic mouse is commonly used to direct genetic recombination in forebrain excitatory neurons. However the original study reported that Emx1-Cre is also expressed in peripheral autonomic ganglia, which could potentially affect the interpretation of targeted circuitry contributing to systemic phenotypes. Here, we report that Emx1- Cre is expressed in nodose ganglion cells whose axon travel within afferent vagal nerves and terminate in the nucleus tractus solitarius (NTS), a critical central autonomic regulatory pathway located in the dorsal medulla. Optogenetic stimulation of Emx1-Cre$^+$ fibers reliably evoked excitatory postsynaptic currents in the NTS in vitro and evoked a parasympathetic bradycardia reflex occasionally with irregular respirations in anesthetized mice *in vivo*. Our study clearly demonstrates that Emx1-IRES-Cre is expressed in the vagal nerve fibers traveling within the central autonomic system involving autonomic cardiorespiratory regulation. These results raise caution when interpreting the systemic phenotypes of Emx1-IRES-Cre conditional recombinant mice, and also suggest the utility of this line to investigate the modulators of afferent vagal system.

Significance Statement

Emx1-IRES-Cre mice are widely used to dissect critical circuitry underlying neurological disorders such as epilepsy. These studies often assume the Cre is expressed selectively only in forebrain excitatory neurons. However, earlier works reported that Emx1 is expressed in several peripheral tissues of the developing embryo and thus gene recombination may affect these peripheral structures. In this study, we characterized the expression and physiological functions of Emx1-Cre expressed in the afferent vagus nerve. Optogenetic stimulation of these Emx1-Cre$^+$ vagus nerves activates the nucleus tractus solitarius neurons within the brainstem *in vitro* and induces brief bradycardia *in vivo*. This study confirmed that peripheral Emx1-Cre$^+$ cells are involved in autonomic regulation and potentially affect transgenic mouse phenotypes.

Abbreviated title: Emx1-Cre expression in the afferent vagus nerve

Introduction

Emx1 is a homeobox gene widely expressed in excitatory neurons in the mammalian forebrain during embryogenesis, including the cerebral cortex, hippocampus, and olfactory bulbs [1,2]. A mouse line carrying Cre recombinase under the endogenous Emx1 promoter (i.e. Emx1-IRES-Cre [1]) has been widely used in studies of neurological diseases to elucidate functions of specific genes in these neurons. In epilepsy studies, developmental Cre-loxP recombination strategy [3] have contributed to the identification of many pathogenic mechanisms of genetic epilepsy [4–8], and some of these studies have suggested that hyperexcitation of Emx1-cre$^+$ forebrain excitatory neurons contribute to premature mortality in epilepsy (SUDEP)[4,6–9] .

Despite the assumption that the Emx1-promoter is specific to forebrain excitatory neurons, earlier studies reported extracerebral expression of Emx1. Endogenous Emx1 is detected in the urogenital tract, branchial pouches, apical ectodermal ridges, and some cranial nerve ganglia of the developing mouse embryo [10], and this expression is reflected in the Emx1-IRES-Cre mouse line [1,11]. Thus when used in the developmental Cre-loxP approach, the functions of the targeted gene expressed in these peripheral cells can be also modulated and might affect overall phenotype, if the gene of interest is expressed. However, the physiological roles of extracerebral peripheral Emx1-cre$^+$ cells are not well characterized in the postnatal mouse.

In this report, we identified that peripheral Emx1-Cre$^+$ cells in the nodose ganglion directly affect cardiorespiratory regulation. Our anatomical study using a fluorescence reporter identified Emx1-Cre expression in their afferent vagal nerve fibers innervating the dorsal medulla. Optogenetic stimulation of these Emx1-Cre$^+$ afferent fibers in acutely prepared brainstem slices *in vitro* confirmed functional synapses onto primary neurons within the nucleus tractus solitarius (NTS), and trigger parasympathetic bradycardia in anesthetized mouse preparations *in vivo*. The ascending projection from NTS neuron has a complex influence on forebrain functions involved in somatic and autonomic systems. These results raise caution when interpreting behavioral and neurophysiological phenotypes of transgenic mice using the Emx1-IRES-Cre line.

Material and Methods

Animals

All animal experiments were conducted under the protocol approved by the Baylor College of Medicine IACUC and conducted in accordance with the *Guide* of AAALAC. Emx1-IRES-Cre (Emx1-Cre, JAX stock number: 005628), floxed-ChR2 (Ai32, JAX stock number: 012569), and floxed-tdtomato (Ai9, JAX stock number: 007909) lines were obtained from Jackson laboratory. These animals were crossed and maintained in the vivarium with standard mouse chow. Experiments were conducted on animals aged P25-90. We initially conducted studies using male and female mice separately. However because we did not detect major differences in Cre expression patterns, and both male and female mice data were pooled.

Fluorescence imaging

Adult Emx1-cre:tdtomato mice were transcardially perfused with PBS followed by 4% formalin. Brains were extracted and kept in 4% formalin overnight at 4°C, then transferred to 30% sucrose solution until the brain sinks. Fixed brains were frozen in OTC, cut in 20 µm sagittal or coronal sections, and mounted on glass slides. After washing in PBS, sections were coverslipped with a mounting medium (Prolong gold antifade) and analyzed on a microscope (Keyence). In the higher magnification image shown in **Figure 1F**, the image was de-blurred using a deconvolution algorithm.

The nodose ganglion and vagus nerve were also extracted from formalin-fixed mice and incubated in 4% formalin overnight at 4°C. A whole-mount tissue was placed on a glass slide, and differential interference contrast (DIC) and fluorescence images were acquired. In some experiments, the nodose microstructure was cut in 10 µm frozen sections to characterize their microstructures. In **Figure 2B**, the background fluorescence signal was eliminated by adjusting the threshold.

Brainstem slice preparation

Acute brainstem slices were prepared as described previously [12]. Briefly, mice were deeply anesthetized with a mixture of ketamine/xylazine (35 mg/75 mg per kg mouse, i.p.), transcardially perfused with dissection solution (110 mM N-Methyl-D-glucamine HCl (pH 7.4), 8 mM $MgSO_4$, 25 mM $NaHCO_3$, 1.25 mM Na_2HPO_4, 3mM KCl, 10 mM glucose, 0.4 mM sodium ascorbate, saturated with 95%

O_2/5% CO_2 gas), decapitated, the brain extracted, and 200 µm coronal slices were cut using a vibratome (Leica VT1200S). Slices were recovered in dissection solution at 33°C for 10 minutes, then transferred and kept in artificial cerebrospinal fluid (ACSF: 130 mM NaCl, 3 mM KCl, 25 mM $NaHCO_3$, 1.25 mM Na_2HPO_4, 10 mM glucose, 0.4 mM sodium ascorbate, saturated with 95% O_2/5% CO_2 gas) at room temperature until transferred to the experimental chamber.

In vitro electrophysiology of nucleus tractus solitarius (NTS) neurons

Whole-cell recordings were made from visually identified NTS neurons. The recording chamber was continuously superfused with ACSF at 2.5-3.0 mm/min and maintained within 33-34°C. The recording pipette contained Cs-gluconate based internal solutions (in mM: 130 gluconic acid, 10 HEPES, 1 $MgCl_2$, 8 NaCl, 10 BAPTA, 5 TEA-Cl, 5 QX314, 2 Mg-ATP, 0.3 Na-GTP, pH adjusted to 7.2 with CsOH). Evoked EPSCs were recorded at -70mV and 0mV after correcting for a 10 mV of measured liquid junction potential. EPSCs were evoked by photostimulation of surrounding tissue using a 200 µm diameter silicon tip LED (Thorlabs), delivered for 10 ms, at 20 Hz, for 10 times. Stimulation strength was adjusted to obtain minimum responses and was typically within 0.5-1.5 mW. Signals were amplified with a Multiclamp 700B amplifier, digitized, and analyzed using pClamp10 software (Molecular instruments). The individual EPSCs were detected based on a template search and events >4 pA were included.

Cardiorespiratory response to optogenetic vagal afferent stimulation in the anesthetized mouse

Emx1-IRES-Cre:ChR2 mice (~P40) was anesthetized with urethane (1.2-1.5 mg/kg, i.p.), allowing spontaneous respiration. Body temperature was maintained at 36.5-37.0˚C using a feedback heating blanket and rectal thermistor. Oxygen saturation level (SpO_2) was periodically tested from a depilated left thigh using the MouseOx sensor (Starr life science) and was always above 97.5% throughout the experiments. A pair of needle electrodes were inserted into the thoracic wall for electrocardiography, and a piezo disc was placed under the abdomen to detect breathing. Physiological signals were amplified using a Bioamp, digitized, and analyzed using the Labchart system (ADI). After achieving a state of stable anesthesia, hair covering the dorsal neck was removed, the skin was cleansed, and a midline incision was made to expose the occipital bone. The neck muscles were carefully separated, a part of the occipital bone and ligament was removed to expose the surface of dorsal medulla (**Figure 4A**). An LED fiber (1.25 mm tip size, 200 µm core diameter) connected with a spacer was placed over

the dorsal brainstem surface and photostimulation was delivered using an LED power controller (LEDD1B, Thorlabs) and Master 8 (AMPI). The parameter used for stimulation was 20 Hz and 10 ms and 100 pulses were delivered. Typical stimulation power was within 2.0-2.5 mW. The stimulation site was adjusted to obtain optimal responses. Once the baseline response was determined, the mouse was injected with atropine (1 mg/kg, i.p.) to block parasympathetic activity.

Drugs

Atropine and other chemicals were purchased from Sigma Aldrich.

Results

Emx1-Cre is expressed in afferent vagal nerve terminals within the nucleus tractus solitarius in the brainstem medulla

We characterized the distribution of Emx1-Cre expression by crossing Emx1-IRES-Cre with floxed-tdtomato mice (hereafter Emx1-tdtomato). Emx1-Cre driven tdtomato expression in the cerebral cortex was obvious due to the gross pink coloration of the tissues. The cortico-spinal tract was detected as a faint pink line running along the midline of the ventral brainstem. In sagittal sections, a strong fluorescence signal was obvious in forebrain structures (Figure 1A) as well as in the diencephalon due to corticofugal projections. We observed significant Emx1-tdtomato expression within the brainstem with circumscribed regions of expression seen in the dorsal pons/medulla (**Figure 1 C-F**).

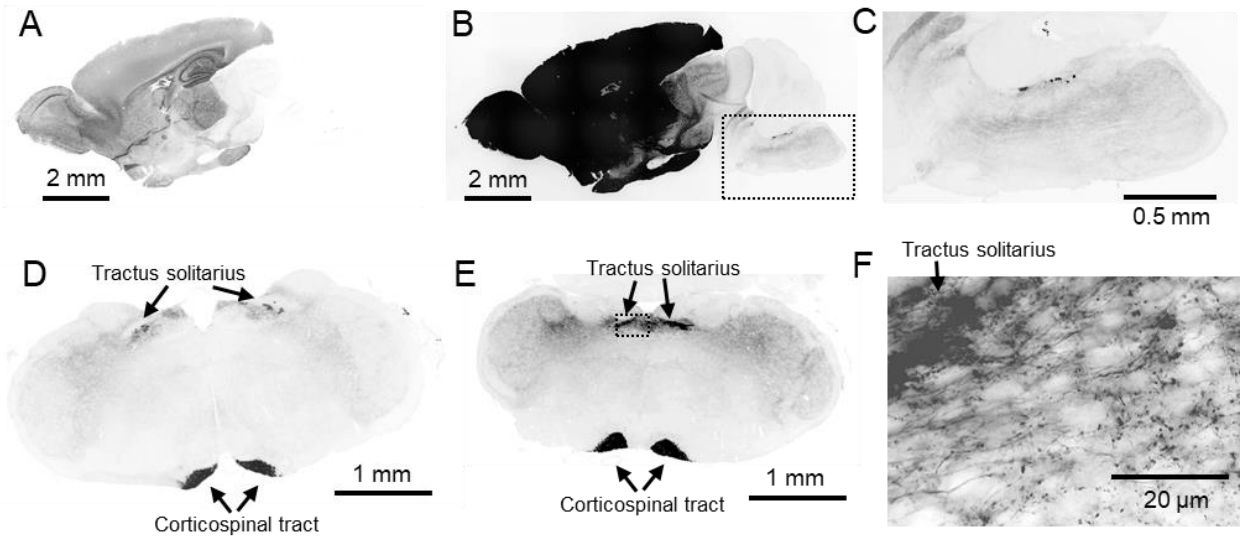

Figure 1. Characterization of Emx1-tdtomato signals in the brain. The fluorescence signal is inverted and shown in black color. **A-C** A midsagittal section showing strong fluorescence in forebrain structures. Overexposed image in **B** shows minor but significant signals present in hindbrain regions. The box in B is enlarged in **C**. **D-F** Coronal sections of Rostral (**D**) and caudal (**E**) medulla. Fluorescence signals were present in the tractus solitarius and corticospinal tract. The box in **E** is shown enlarged in **F**. Dense fluorescence is present in the tractus solitarius, and labeled single axonal fibers with varicosities are detected in the NTS filed.

In order to identify the origin of brainstem Emx1-Cre$^+$ signals, we next analyzed a series of coronal sections. A strong signal was detected in the medial ventral area corresponding to the cortico-spinal tract (**Figure 1D&E**). Fluorescence signals were also detected in the dorsal medulla within the nucleus of tractus solitarius (NTS). In high magnification images, these were identified as fine fibers with axonal varicosities originating from tractus solitarius (**Figure 1F**), the afferent vagal innervation. The signals

were enriched within the NTS, while sparse axon fibers innervated the lateral structures involving the trigeminal nucleus. We did not observe any fluorescent cellular somata in this area.

We next investigated Emx1-tdtomato expression in the cranial ganglia and visceral organs. The resected whole nodose ganglion (**Figure 2A**), where the majority of afferent vagus nerves originate, showed tdtomato fluorescence (**Figure 2B-D**). The fluorescence signal was barely visible in the vagus nerve at low magnification likely due to the high light refraction of the ensheathing myelin. Within the nodose ganglion, Emx1-tdtomato signals were detected in the soma as well as in the nerve fibers of ganglion cells (**Figure 2E**). These results confirmed the Emx1-Cre expression in the sensory vagal neurons.

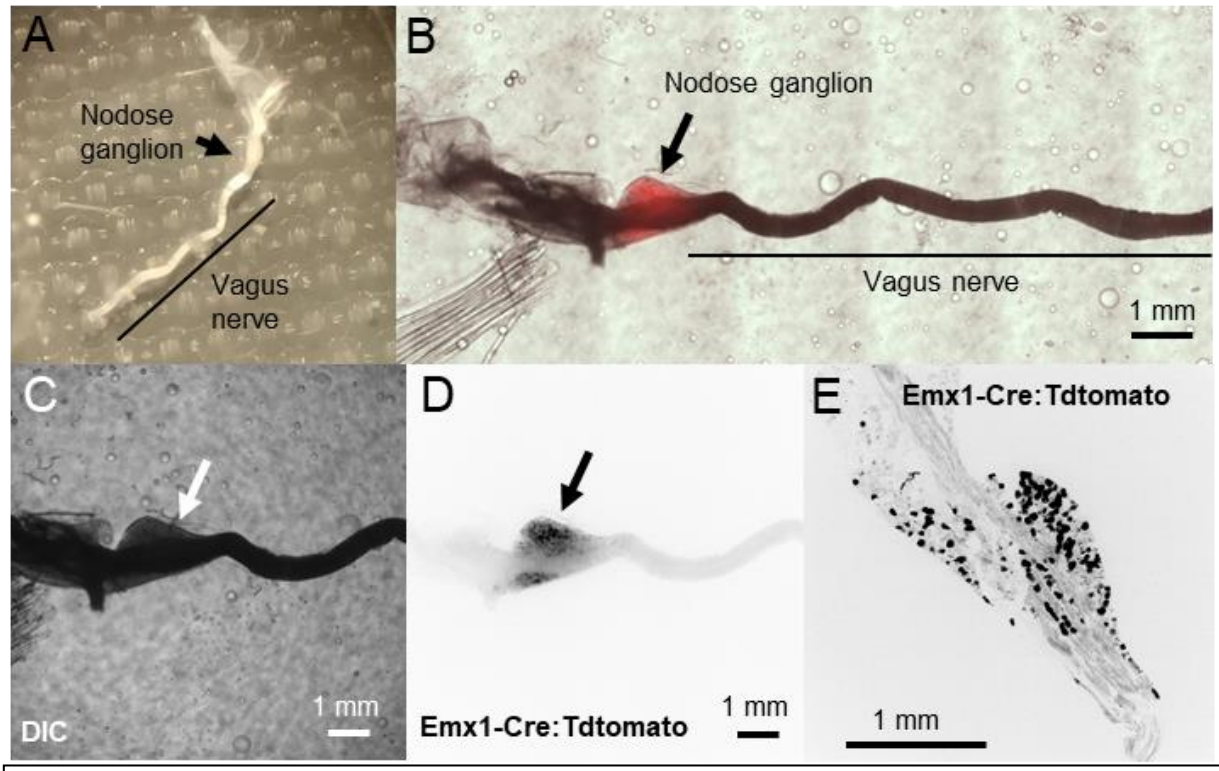

Figure 2. Characterization of Emx1-tdtomato signals in the nodose ganglion. **A.** Dissected nodose ganglion on the vagus nerve. **B.** Pseudocolor image merging DIC (**C**) and tdtomato fluorescence (**D**) images of whole mount nodose ganglion. **E.** high magnification image of sectioned nodose ganglion Note fluorescence signals in **D&E** are inverted and shown in black

Emx1-tdtomato signal was also observed in the salivary glands and kidney (not shown), the latter is consistent with an earlier study that reported endogenous Emx1 expression in the urinary tract during development. Macroscopic observation did not detect visible expression of Emx1-tdtomato in isolated heart or lungs, while we do not exclude possible expression in their microstructures.

Together, our anatomical study revealed a significant expression of Cre-mediated recombination in extracerebral structures of the postnatal Emx1-IRES-Cre mouse. Because of their neuronal gene expression and the relevance to autonomic dysfunctions and premature death reported in studies using Emx1-IRES-Cre mice, we further characterized the physiological functions of the Emx1-Cre$^+$ vagus afferent nerve.

Emx1-Cre$^+$ vagus nerve terminals excite neurons within the nucleus tractus solitarius (NTS)

In order to test the physiological functions of Emx1-Cre$^+$ afferent vagus nerve, we crossed Emx1-IRES-cre mice with floxed-channelrhdopsin (ChR2) and characterized synaptic function using acutely prepared brainstem slices containing the NTS *In vitro*. Whole-cell recordings were made from the visually identified NTS neurons which receive monosynaptic input from the afferent vagal nerves (tractus solitarius, **Figure 3A**). Trains of photo-stimulations (10 ms, 20 Hz, 10 pulses) reliably triggered excitatory postsynaptic currents (EPSCs) in the recorded NTS neurons with minimal variability in latency (**Figure 3B&D**), suggestive of a monosynaptic connection [13]. The evoked EPSCs were detected in all recorded NTS neurons (n=27 cells, 3 mice), suggesting that the majority, if not all, of the afferent vagus nerve fibers that synapse onto NTS neurons express Emx1-Cre during development. No responses were detected when photostimulation was tested in mice without ChR2 (10 cells, 3 mice).

The vagus afferent nerves are comprised of TRPV1$^+$ and TRPV1$^-$ fibers as characterized by the presence or absence of asynchronous presynaptic glutamate release, respectively [13,14], and each NTS neuron receives only one of either type of afferent input. We grouped asynchronous and synchronous release populations based on the presence of increased sEPSCs during the 1 s post-stimulation period. With this criterion, we identified cell groups with synchronous (30%, 8/27 cells **Figure 3 B&C**) and asynchronous release (70%, 19/27 cells **Figure 3 D&E**). This result suggests that Emx1-Cre is likely expressed in both types of vagal afferent cell populations.

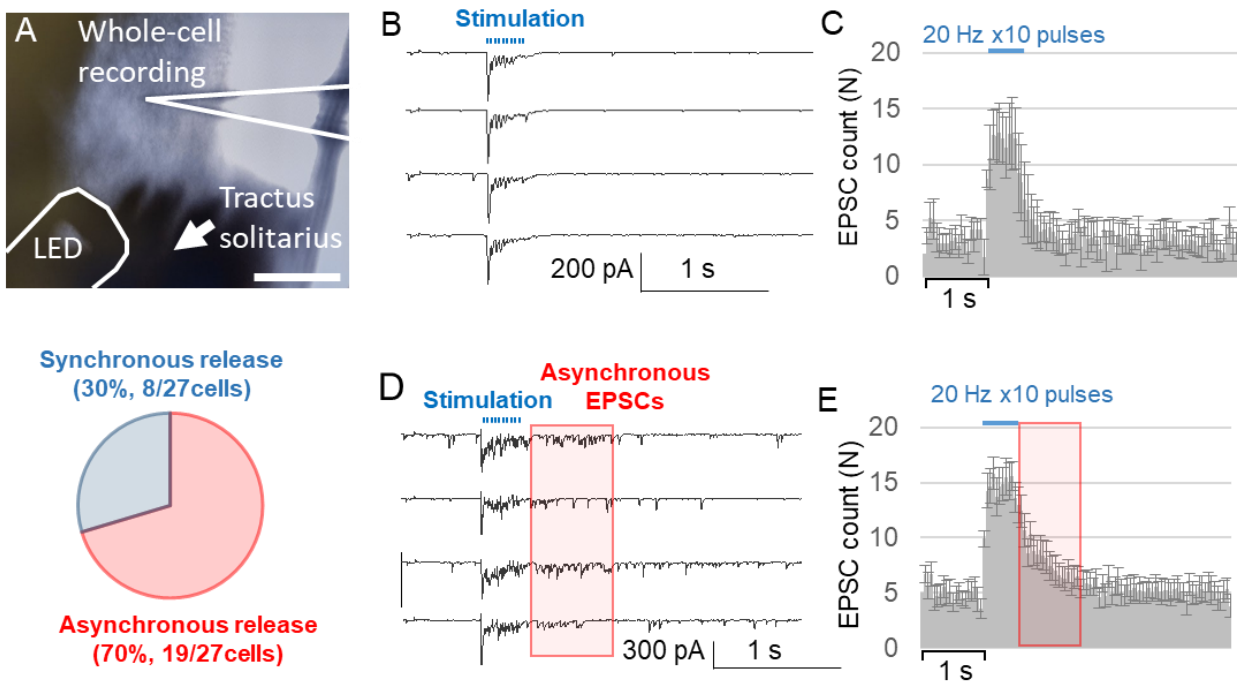

Figure 3. Optogenetic stimulation of Emx1-Cre^{+} nerve fibers *in vitro*. Vagus afferent nerve (tractus solitarius) was stimulated by LED located overt the slice (**A**). Scale: 200 µm. Photostimulation evoked either synchronous (**B&C**) or asynchronous EPSCs (**D&E**) in all recorded NTS neurons (n=27). 30% (8/27) of NTS neurons showed synchronous, whereas 70% (19/27) of neurons received asynchronous EPSCs. **B&D** representative EPSC traces and **C&E** Histograms of mean EPSC (50 ms bins). Note the elevation of EPSC frequency following optogenetic afferent stimulation in **E**. values are mean ± standard error

Optogenetic stimulation of Emx1-Cre^{+} afferent vagus nerve triggers bradycardia in the anesthetized mouse

Finally, we examined the physiological function of the Emx1^{+} afferent nerve *in vivo* using a urethane anesthetized mouse preparation. The dorsal medulla was exposed by removing the overlying neck muscles and dura, and a LED was positioned to target the dorsal medulla with a spacer to avoid direct tissue contact (~1-2 mm distance, **Figure 4A**). Optogenetic stimulation (20 Hz, 100 pulses) of the dorsal medulla evoked fast bradycardia in these mice which was occasionally associated with irregular respirations (**Figure 4C**). In some recordings, secondary late bradycardia was observed (**Figure 4C**). The bradycardia response was always transient and recovered even when stimulation was continued. No responses were detected in Emx1-ChR2$^{-/-}$ control mice.

Atropine (0.5-1 mg/kg, i.p.), a muscarinic receptor antagonist, effectively abolished the fast evoked cardiac depression response, indicating recruitment of a parasympathetic mechanism. On the other hand, the late bradycardia was not affected by atropine, suggesting a mechanism other than parasympathetic involvement can be recruited in some experiments. Because of infrequent detection of the late secondary response, we did not further characterize this phenomenon.

These results indicate that the Emx1-Cre positive vagal afferent nerve is involved in central autonomic cardiac and respiratory regulation and genetic manipulation of their excitability may alter the autonomic circuit stability.

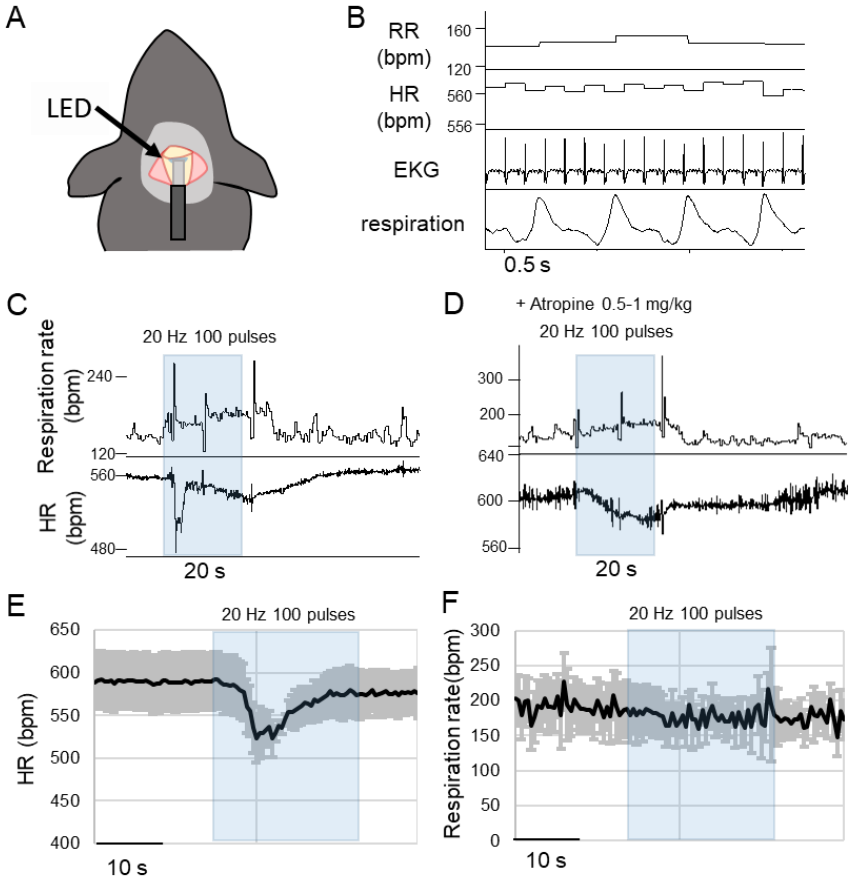

Figure 4. Optogenetic stimulation of Emx1-Cre^{+} nerve fibers *in vivo* urethane anesthetized mouse. **A** Recording configuration. An LED was horizontally positioned over the exposed dorsal medulla surface. A spacer was used to prevent direct contact. **B.** Heart rate and respiration were converted to instantaneous frequency. C. stimulation triggered a complex bradycardia associated with respiratory irregularity. D. The fast response was eliminated by the anticholinergic drug atropine. **E&F** Mean traces of heart rate (**E**) and respiration responses (**F**) to stimulation. n=5 responses, values are mean ± standard error

Discussion

In this study, we characterized the central afferent vagal nerve expressing Emx1-IRES-Cre, a Cre diver line commonly used to investigate the impact of forebrain excitatory neurons on neurological phenotypes. Consistent with previous studies, we found Emx1-Cre expression in peripheral organs, including the nodose ganglion where parent cell bodies giving rise to central vagus afferent nerve are located. Our electrophysiological characterization confirmed that these nerve terminals form functional synapses with NTS neurons in the dorsal medulla and are involved in cardiorespiratory regulation. Thus, even when the phenotype of an Emx1-IRES-Cre based mutant mouse recapitulates a specific genetic disease, the phenotype cannot be solely attributed to forebrain excitatory neurons if the gene of interest is also expressed in the peripheral sites.

Endogenous Emx1 expression in the dorsal telencephalon has been detected as early as E9.5 [2], thus the Emx1-IRES-Cre line is useful for characterization of neonate/pediatric genetic diseases which arise during prenatal circuit maldevelopment. However, Emx1 is also detected in peripheral tissues including branchial pouches, kidneys, developing limb appendages, and autonomic ganglia (VII, VIII, X, and XI) of developing mouse embryo [1]. While these peripheral expressions may be only transient during development, Cre-loxP recombination permanently alters the target gene expression in these structures. Our results confirmed that the embryonic Emx1 expression patterns are carried over into the postnatal adult mouse using Emx1-IRES-Cre:tdtomato reporter line.

This study focused on the afferent vagus nerve system because they share neuronal genes expressed in excitatory neurons such as Kv1.1, Kcnq2, Kcnq3, Scn1a, Scn8a [15–19], genes that are relevant to epilepsy. Comprehensive gene expression of vagal sensory neurons in the nodose ganglion has been identified by transcriptomic analysis [16]. On the other hand, omics study can failed to reveal enrichment of genes such as Kcnq2 and Kv1.6, despite their potential roles in shaping the axonal excitability [17,18]. Other genes implicated in genetic neurological diseases may also be present at low abundance in the vagal neurons, and modulation of their expression may affect central autonomic regulation.

Our study found that optogenetic stimulation of the vagus afferent nerve activates the majority of NTS neurons *in vitro* and induces a transient cardio-depression *in vivo* under urethane anesthesia. Both of these responses were transient in nature; optogenetically evoked EPSC trains showed a progressive decrease in their amplitude (**Figure 3**) which is consistent with the response evoked by electrical stimulation [14], and optogenetic stimulation could only evoke a ~10 s lasting transient period of bradycardia even when stimulation was continued longer time (**Figure 4**). Thus Emx1-cre^{+} circuits are

normally involved in the rapidly sensitize reflex circuits, and sustained bradycardia seen in the pathological situation may require recruitment of additional neuromodulatory pathways such as tissue hypoxia[20] and metabotropic receptor mechanisms [21]. In contrast to consistent cardiac responses, respiratory changes in response to optogenetic stimulation were inconsistent and did not produce a significant change when averaged (**Figure 4F**). We do not know the underlying cause of such inconsistency, but it may partly be explained by a minor difference in the stimulation sites or depth of anesthesia in each animal. In fact, while urethane has a relatively small impact on cardiorespiratory reflex system, it still blunts the dynamic range [22,23]. In this regard, the physiological properties of Emx1-Cre$^+$ vagal nerves may be better appreciated in awake animal models.

This study focused on cardiorespiratory effects of the Emx1-Cre$^+$ vagus nerve activation, however, afferent vagal nerves carry visceral interoceptive signals which are received by NTS neurons and are propagated not only to autonomic circuitries within the hypothalamus and brainstem, but also forebrain structures, directly and indirectly [24,25]. These broad and bilateral central projections have been invoked to explain the therapeutic effects of vagus nerve stimulation across a range of neuropsychiatric disorders, including major depression and epilepsy. Thus modulation of afferent vagal nerve excitability by Emx1-Cre may also affect cortical hyperexcitability and neurobehavioral phenotypes.

In addition to Emx1, a similar technical concern may be present in parvalbumin (PV)-Cre mouse line, frequently used to target fast-spiking interneurons. In fact, PV is known to be expressed in the nodose and petrosal ganglia [26,27], diaphragm [28], and renal tubes [29]. The functional significance of these peripheral PV$^+$ cells in autonomic physiology remains to be elucidated.

Together, the present study establishes the functional role of Emx1-Cre$^+$ cells in the regulation of cardiorespiratory function. Caution is needed when interpreting alteration in systemic physiology resulting from developmental Cre-flox transgenic mouse studies using this Cre driver line.

Acknowledgments

We thank Drs Krishnan and Maheshwari for helpful comments on this manuscript.

Funding sources

This work was supported by American Heart Association career development grant 19CDA34660056 (I.A.), Curtis Hankamer Basic Research Fund at Baylor College of Medicine (IA), American Epilepsy Society Junior Investigator Award (IA), NIH Center for SUDEP Research (NS090340, J.L.N), and Blue Bird Circle Foundation (J.L.N.).

References

1. Gorski, J. A. *et al.* Cortical excitatory neurons and glia, but not GABAergic neurons, are produced in the Emx1-expressing lineage. *J Neurosci* **22**, 6309–6314 (2002).
2. Simeone, A. *et al.* Two vertebrate homeobox genes related to the Drosophila empty spiracles gene are expressed in the embryonic cerebral cortex. *EMBO J* **11**, 2541–2550 (1992).
3. Orban, P. C., Chui, D. & Marth, J. D. Tissue- and site-specific DNA recombination in transgenic mice. *Proc Natl Acad Sci U S A* **89**, 6861–6865 (1992).
4. Boillot, M. *et al.* Glutamatergic neuron-targeted loss of LGI1 epilepsy gene results in seizures. *Brain* **137**, 2984–2996 (2014).
5. Makinson, C. D. *et al.* Regulation of Thalamic and Cortical Network Synchrony by Scn8a. *Neuron* **93**, 1165-1179.e6 (2017).
6. Soh, H., Pant, R., LoTurco, J. J. & Tzingounis, A. V. Conditional deletions of epilepsy-associated KCNQ2 and KCNQ3 channels from cerebral cortex cause differential effects on neuronal excitability. *J. Neurosci.* **34**, 5311–5321 (2014).
7. Ishida, S. *et al.* Dorsal telencephalon-specific *Nprl2* - and *Nprl3* -knockout mice: novel mouse models for GATORopathy. *Human Molecular Genetics* ddab337 (2021) doi:10.1093/hmg/ddab337.
8. Klofas, L. K., Short, B. P., Zhou, C. & Carson, R. P. Prevention of premature death and seizures in a Depdc5 mouse epilepsy model through inhibition of mTORC1. *Human Molecular Genetics* ddaa068 (2020) doi:10.1093/hmg/ddaa068.

9. Bunton-Stasyshyn, R. K. A. *et al.* Prominent role of forebrain excitatory neurons in SCN8A encephalopathy. *Brain* **142**, 362–375 (2019).

10. Briata, P. *et al.* EMX1 homeoprotein is expressed in cell nuclei of the developing cerebral cortex and in the axons of the olfactory sensory neurons. *Mech Dev* **57**, 169–180 (1996).

11. Zhou, J. *et al.* Comparison of the Spatiotemporal Expression Patterns of Three Cre Lines, Emx1IRES-Cre, D6-Cre and hGFAP-Cre, Commonly Used in Neocortical Development Research. *Cereb Cortex* bhab305 (2021) doi:10.1093/cercor/bhab305.

12. Aiba, I. & Noebels, J. L. Spreading depolarization in the brainstem mediates sudden cardiorespiratory arrest in mouse SUDEP models. *Sci Transl Med* **7**, 282ra46 (2015).

13. Peters, J. H., McDougall, S. J., Fawley, J. A. & Andresen, M. C. TRPV1 marks synaptic segregation of multiple convergent afferents at the rat medial solitary tract nucleus. *PLoS One* **6**, e25015 (2011).

14. Peters, J. H., McDougall, S. J., Fawley, J. A., Smith, S. M. & Andresen, M. C. Primary afferent activation of thermosensitive TRPV1 triggers asynchronous glutamate release at central neurons. *Neuron* **65**, 657–669 (2010).

15. Glasscock, E., Qian, J., Kole, M. J. & Noebels, J. L. Transcompartmental reversal of single fibre hyperexcitability in juxtaparanodal Kv1.1-deficient vagus nerve axons by activation of nodal KCNQ channels. *J Physiol* **590**, 3913–3926 (2012).

16. Kupari, J., Häring, M., Agirre, E., Castelo-Branco, G. & Ernfors, P. An Atlas of Vagal Sensory Neurons and Their Molecular Specialization. *Cell Rep* **27**, 2508-2523.e4 (2019).

17. Glazebrook, P. A. *et al.* Potassium channels Kv1.1, Kv1.2 and Kv1.6 influence excitability of rat visceral sensory neurons. *J Physiol* **541**, 467–482 (2002).

18. Sun, H. *et al.* KCNQ/M-channels regulate mouse vagal bronchopulmonary C-fiber excitability and cough sensitivity. *JCI Insight* **4**, (2019).

19. Kollarik, M. *et al.* Different role of TTX-sensitive voltage-gated sodium channel (NaV 1) subtypes in action potential initiation and conduction in vagal airway nociceptors. *J Physiol* **596**, 1419–1432 (2018).

20. Kim, Y. *et al.* Severe peri-ictal respiratory dysfunction is common in Dravet syndrome. *J Clin Invest* **128**, 1141–1153 (2018).

21. Aiba, I. & Noebels, J. L. Adrenergic agonist induces rhythmic firing in quiescent cardiac preganglionic neurons in nucleus ambiguous via activation of intrinsic membrane excitability. *J Neurophysiol* **121**, 1266–1278 (2019).

22. Massey, C. A. & Richerson, G. B. Isoflurane, ketamine-xylazine, and urethane markedly alter breathing even at subtherapeutic doses. *J Neurophysiol* **118**, 2389–2401 (2017).

23. Sapru, H. N. & Krieger, A. J. Cardiovascular and respiratory effects of some anesthetics in the decerebrate rat. *Eur J Pharmacol* **53**, 151–158 (1979).

24. Kawai, Y. Differential Ascending Projections From the Male Rat Caudal Nucleus of the Tractus Solitarius: An Interface Between Local Microcircuits and Global Macrocircuits. *Front. Neuroanat.* **12**, 63 (2018).

25. Naritoku, D. K., Terry, W. J. & Helfert, R. H. Regional induction of fos immunoreactivity in the brain by anticonvulsant stimulation of the vagus nerve. *Epilepsy Res* **22**, 53–62 (1995).

26. Ichikawa, H. & Helke, C. J. Parvalbumin and calbindin D-28k in vagal and glossopharyngeal sensory neurons of the rat. *Brain Res* **675**, 337–341 (1995).

27. Sato, D. *et al.* Distribution of TRPVs, P2X3, and parvalbumin in the human nodose ganglion. *Cell Mol Neurobiol* **34**, 851–858 (2014).

28. Jeckel-Neto, E. A., Ito, Y., Sato, T. & Tauchi, H. Quantitative immunohistochemistry of parvalbumin expression in the rat diaphragm. *Anal Quant Cytol Histol* **15**, 201–205 (1993).

29. Belge, H. *et al.* Renal expression of parvalbumin is critical for NaCl handling and response to diuretics. *Proc Natl Acad Sci U S A* **104**, 14849–14854 (2007).